

On the Maximal Number of Real Embeddings of Spatial Minimally Rigid Graphs

Evangelos Bartzos^{1,2}, Ioannis Emiris^{1,2}, Jan Legerský³, and Elias Tsigaridas⁴

¹Department of Informatics and Telecommunications, National Kapodistrian University of Athens

²ATHENA Research Center

³Research Institute for Symbolic Computation, Johannes Kepler University, Linz

⁴Sorbonne Université, CNRS, INRIA, Laboratoire d'Informatique de Paris 6 (LIP6), Équipe POLSYS

Abstract

The number of embeddings of minimally rigid graphs in \mathbb{R}^D is (by definition) finite, modulo rigid transformations, for every generic choice of edge lengths. Even though various approaches have been proposed to compute it, the gap between upper and lower bounds is still enormous. Specific values and its asymptotic behavior are major and fascinating open problems in rigidity theory.

Our work considers the maximal number of real embeddings of minimally rigid graphs in \mathbb{R}^3 . We modify a commonly used parametric semi-algebraic formulation that exploits the Cayley-Menger determinant to minimize the *a priori* number of complex embeddings, where the parameters correspond to edge lengths. To cope with the huge dimension of the parameter space and find specializations of the parameters that maximize the number of real embeddings, we introduce a method based on coupler curves that makes the sampling feasible for spatial minimally rigid graphs.

Our methodology results in the first full classification of the number of real embeddings of graphs with 7 vertices in \mathbb{R}^3 , which was the smallest open case. Building on this and certain 8-vertex graphs, we improve the previously known general lower bound on the maximum number of real embeddings in \mathbb{R}^3 .

1 Introduction

Rigid graph theory is a very active area of research with many applications in robotics [13, 31, 32], structural bioinformatics [10, 21], sensor network localization [33] and architecture [12].

A graph embedding in \mathbb{R}^D , equipped with the standard euclidean norm, is a function that maps the vertices of a graph G to \mathbb{R}^D . Let V_G , resp. E_G , denote the set of vertices, resp. edges, of G . We are interested in embeddings that are compatible with edge lengths, namely, if two vertices are connected by an edge, then the distance between them equals a given length for this edge. A graph G is *generically rigid* if all embeddings compatible with generic edge lengths are not continuously deformable. If any edge removal results in a non-rigid mechanism, then the graph is *minimally rigid*. For $D = 2$ these graphs are called *Laman graphs*. For $D = 3$, following [15], we call these graphs *Geiringer graphs* to honor Hilda Pollaczek-Geiringer who worked on rigid graphs in \mathbb{R}^2 and \mathbb{R}^3 many years before Laman [25, 24].

For a graph G , let $r_D(G, \mathbf{d})$ be the number of embeddings in \mathbb{R}^D that are compatible with edge lengths $\mathbf{d} = (d_e)_{e \in E_G} \in \mathbb{R}_+^{|E_G|}$ modulo rigid motions, and let $r_D(G)$ be the maximum of $r_D(G, \mathbf{d})$ over all \mathbf{d} such that $r_D(G, \mathbf{d})$ is finite. To indicate the maximum number of real embeddings over all graphs with n vertices, we write $r_D(n)$. In this setting, an important question is to find all the possible real embeddings of graphs with k (some constant) number of vertices. This can be used to enumerate and classify conformations of proteins, molecules [10, 21] and robotic mechanisms, e.g., [32, 8]. Furthermore, precise bounds for $r_D(G)$ or $r_D(k)$ are of great importance, since gluing many copies of G together yields lower bounds for $r_D(n)$, for $n \geq k$, e.g., [5, 15].

A natural approach to bound $r_D(G)$ is to use an algebraic formulation to express the embeddings as solutions of a polynomial system. The number of its complex solutions bounds the number of complex embeddings, $c_D(G)$, which bounds $r_D(G)$.

For $D = 2$, there is a recent algorithm [6] to solve the problem of complex embeddings, $c_2(G)$, of minimally rigid graphs in \mathbb{C}^2 , for any given graph G . Besides this graph-specific approach, using determinantal varieties [4, 5] we can estimate asymptotic bounds, see also [11, 28]; this approach also gives results for $D = 3$. Complex bounds for certain cases of Laman graphs are also given in [18]. For graphs with a constant number of vertices, we know that $r_2(6) = 24$, where the proof technique uses the coupler curve of the Desargues graph [5], and $r_2(7) = 56$, proved by delicate stochastic methods [9]. The second bound yields the best known lower bound for Laman graphs, which is $r_2(n) \geq 2.3003^n$.

For $D = 3$, the problem is much more difficult than in the planar case. One of the reasons is that, unlike the planar case, we lack a combinatorial characterization of minimally rigid (Geiringer) graphs in \mathbb{R}^3 . The existence of such a characterization is a major open problem in rigid graph theory. The algebraic formulation considers the squared distance between two points, not as a metric, but as the sum of squares of the coordinates. Then, for every edge $v_i v_j$, we have the equation

$$d_{ij}^2 = (x_i - x_j)^2 + (y_i - y_j)^2 + (z_i - z_j)^2,$$

where x_i, y_i, z_i are, in general complex, coordinates of a vertex v_i and d_{ij} is the length of the edge $v_i v_j$. If we use the Bézout bound to bound the number of the complex roots of the polynomial system, then the upper bound for $c_3(n)$ is $\mathcal{O}(2^{3n})$, which is a very loose bound. Hence, a more sophisticated approach is needed. Nevertheless, this formulation has been successfully used to obtain upper bounds of $r_3(k)$ via mixed volume computation of sparse polynomial systems for 1-skeleta of simplicial polyhedra (a subset of spatial rigid graphs) with $k \leq 10$ vertices [11]. The best known lower bound is $r_3(n) \geq 2.51984^n$ [11]. We improve it to 2.6553^n .

As our goal is to estimate the number of real embeddings, we are interested in the number of real solutions of the corresponding polynomial systems. If we consider the edge lengths as parameters, then we are searching for specializations of the parameters that maximize the number of real solutions of the system and, if possible, to match the number of complex solutions. However, the number of parameters is very big even for graphs with a small number of vertices. Even more, it is an open question in real algebraic geometry to determine if the number of real solutions of a given algebraic system is the same as the number of complex ones up to its parameters. While there are some upper bounds for the number of real positive roots [27], they are generally worse than mixed volume in the case of rigid embeddings. In addition, sparse polynomials have also been used to obtain lower bounds of the number of real positive roots of polynomial systems, see [1, 2] and references therein. Therefore, we need a delicate method to sample in an efficient way the parameter space and maximize the number of real solutions that correspond to embeddings.

For graphs with a given number of vertices, we have a complete classification for all graphs with $n \leq 6$ vertices. Moreover, for the case of the cyclohexane we know the tight bound of $r_3(6) = 16$ embeddings [10]. Let us also mention that for certain applied cases there are ad

hoc methods. For example, the maximal number of real embeddings of Stewart platforms was computed [8] using a combination of Newton-Raphson and the steepest descent method.

Our contribution We extend existing results about the number of the spatial embeddings of minimally rigid graphs. We construct all minimally rigid graphs up to 8 vertices and we classify them according to the last Henneberg step. Then, we model our problem algebraically using two different approaches. Using the algebraic formulation, we compute upper bounds for the number of complex embeddings of all graphs with 7 and 8 vertices. Then, we introduce a method, inspired by coupler curves, to search efficiently for edge lengths that increase the number of real embeddings. We provide an open-source implementation of our method in Python [19], which uses PHCpack [30] for solving polynomial systems. To the best of our knowledge there is no other similar technique, let alone an open-source implementation. Based on our formulation and software, we performed extensive experiments that resulted in a complete classification and tight bounds for the real embeddings for all 7-vertex Geiringer graphs, which was the smallest open case. Moreover, we extend our computations to certain 8-vertex graphs. Even though the computations do not provide a full classification of real embeddings, they are enough to improve the currently known lower bound on the number of embeddings in n , namely $r_3(n) \geq 2.6553^n$.

Organization The rest of the paper is organized as follows. In Section 2 we present the equations and inequalities of our modeling. In Section 3, we introduce a method for parametric searching for edge lengths inspired by coupler curves. In Section 4, we present $r_3(G)$ for all G with 7 vertices and we establish a new lower bounds on the maximum number of real embeddings. Finally, in Section 5 we conclude and present some open questions.

2 Preliminaries & Algebraic Modeling

First, we present some general results about rigidity in \mathbb{R}^3 and then two algebraic formulations of the problem of graph embeddings. The first, in Section 2.2, is based on 0-dimensional varieties of sphere equations. The second, in Section 2.3, exploits determinantal varieties of Cayley-Menger matrices and inequalities.

2.1 Rigidity in \mathbb{R}^3

The first step is the construction of all minimally rigid graphs up to isomorphism for a given number of vertices. The combinatorial characterization of minimally rigid graphs in dimension 3 is a major open problem. It is well known that $|E_G| = 3|V_G| - 6$, and $|E_H| \leq 3|V_H| - 6$ for every subgraph H of G , but this condition is not sufficient for rigidity [26].

It is known that adding a new vertex to a Geiringer graph together with adding and removing certain edges yields another Geiringer graph. These operations are called *Henneberg steps* [29]. Henneberg step I (H1) adds a vertex of degree 3, connecting it with 3 vertices in the original graph. Henneberg step II (H2) deletes an edge from the original graph, a new vertex is connected to the vertices of the deleted edge and to two other vertices of the graph, see Figure 1. For these two steps, the opposite implication also works: If the resulting graph is Geiringer, the original one is Geiringer too. Since the necessary condition for the number of edges guarantees that all Geiringer graphs with ≤ 12 vertices do not have all vertices of degree greater or equal to 5, H1 and H2 are sufficient to construct all Geiringer graphs with ≤ 12 vertices.

There are two additional steps, the so-called X-replacement and double V-replacement (H3x and H3v). They extend rigid graphs in \mathbb{R}^3 with a vertex of degree 5, see Figure 1. Every

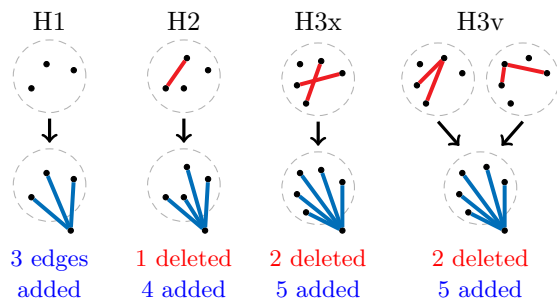


Figure 1: Henneberg steps in \mathbb{R}^3

minimally rigid graph in \mathbb{R}^3 can be constructed by a sequence of steps H1, H2, H3x or H3v starting from a tetrahedron. On the other hand, it is not proven whether these moves construct only rigid graphs [26] (for dimension 4 there is a counterexample such that 4-dimensional variant of H3x gives a non-rigid graph [22]).

2.2 Equations of spheres

Definition 1. If $G = (V_G, E_G)$ is a graph with edge lengths $\mathbf{d} = (d_e)_{e \in E_G} \in \mathbb{R}_+^{|E_G|}$ and $v_1, v_2, v_3 \in V_G$ are such that $v_1v_2, v_2v_3, v_1v_3 \in E_G$, then $S(G, \mathbf{d}, v_1v_2v_3) \subset (\mathbb{C} \times \mathbb{C} \times \mathbb{C})^{|V_G|}$ denotes the zero set of the following equations

$$\begin{aligned} (x_{v_1}, y_{v_1}, z_{v_1}) &= (0, 0, 0), & (x_{v_2}, y_{v_2}, z_{v_2}) &= (0, d_{v_1v_2}, 0), \\ (x_{v_3}, y_{v_3}, z_{v_3}) &= (x_3, y_3, 0), & x_v^2 + y_v^2 + z_v^2 &= s_v \quad \forall v \in V_G, \\ s_u + s_v - 2(x_u x_v + y_u y_v + z_u z_v) &= d_{uv}^2 \quad \forall uv \in E_G, \end{aligned}$$

where x_3, y_3 are such that $x_3 \geq 0$, $x_3^2 + y_3^2 = d_{v_1v_3}^2$ and $x_3^2 + (y_3 - d_{v_1v_2})^2 = d_{v_2v_3}^2$. We denote the real solutions $S(G, \mathbf{d}, v_1v_2v_3) \cap (\mathbb{R} \times \mathbb{R} \times \mathbb{R})^{|V_G|}$ by $S_{\mathbb{R}}(G, \mathbf{d}, v_1v_2v_3)$.

The first 3 equations remove rotations and translations. The distances of vertices from the origin are expressed by new (nonzero) variables to avoid roots at toric infinity which prohibit mixed volume from being tight [11, 28]. The other equations are distances between embedded points.

Notice that $r_3(G, \mathbf{d}) = |S_{\mathbb{R}}(G, \mathbf{d}, v_1v_2v_3)|$. If \mathbf{d} is generic, then $c_3(G, \mathbf{d}) = |S(G, \mathbf{d}, v_1v_2v_3)| = c_3(G)$ since the number of complex embeddings is a generic property. The mixed volume of the system depends on the choice of the fixed triangle. Hence, all possible choices must be tested for some graphs in order to get the best possible bound.

2.3 Distance geometry

Distance geometry is the study of the properties of points given only the distances between them. A basic tool is the squared distance matrix, extended by a row and a column of ones (except for

the diagonal), known as Cayley-Menger matrix [3, Chapter IV, Section 40]:

$$CM = \begin{pmatrix} 0 & 1 & 1 & \cdots & 1 \\ 1 & 0 & d_{12}^2 & \cdots & d_{1n}^2 \\ 1 & d_{12}^2 & 0 & \ddots & \cdots \\ \cdots & \cdots & \ddots & \ddots & \cdots \\ 1 & d_{1n}^2 & d_{2n}^2 & \cdots & 0 \end{pmatrix},$$

where d_{ij} is the distance between point i and j . The points with such distances are embeddable in \mathbb{R}^D if and only if

- $\text{rank}(CM) = D + 2$ and
- $(-1)^k \det(CM') \geq 0$, for every submatrix CM' with size $k + 1 \leq D + 2$ that includes the extending row and column.

The distances among all n points correspond to edge lengths of the complete graph with n vertices. Hence, assuming that lengths of non-edges of our graph G correspond to variables, the first condition gives rise to determinantal equations. This condition suffices for embeddings in \mathbb{C}^D . The systems of these equations are overconstrained (for example 21 equations in 6 variables for $n = 7$ and 56 equations in 10 variables for $n = 8$). The second embedding condition can be interpreted by geometrical constraints on the lengths. For $k = 2$ this means simply that a length should be positive. For $k = 3$ the resulting inequality is the triangular one, while for $k = 4$ we obtain *tetrahedral inequalities*. The latter can be seen as a generalization of the triangular ones, since they state that the area of no triangle is bigger than the sum of the other three in a tetrahedron.

Although the systems of equations are overconstrained, a square subsystem can be found. The question is if these subsystems can give us information for the whole mechanism. In [17], the authors present an idea relating Cayley-Menger subsystems with *globally rigid* graphs. They are a certain class of graphs consisting of mechanisms with unique realizations up to rigid motions and reflections. If extending G by the edges corresponding to the variables of the square subsystem yields a globally rigid graph, then the number of solutions of the reduced system gives an upper bound for the whole system. Since the reflections are factored out by the distance system, the number of solutions is $c_3(G)/2$. We check global rigidity using stress matrices derived from rigidity matroids [14].

It is easy to find square subsystems from the determinantal equations. The question is what is the smallest number of variables needed to establish an upper bound and if this subsystem captures all solutions of the whole graph. The following lemma provides an estimate of the number of variables.

Lemma 1. *For every minimally rigid graph G in dimension 3, there is at least one extended graph $H = G \cup \{e_1, e_2, \dots, e_k\}$, with $k = |V_G| - 4$ and $e_i \notin E_G$, which is globally rigid in \mathbb{C}^3 .*

Proof. The only 5-vertex minimally rigid graph is obtained by applying an H1 step to the tetrahedron. If we extend this graph with the only non-existing edge, we obtain the complete graph in 5 vertices, so the lemma holds. Let the lemma hold for all graphs with n or less vertices. For every graph obtained by an H2 step, the lemma holds since H2 preserves global rigidity [7].

Let a graph G_{n+1} be constructed by an H1 move applied to an n -vertex graph G_n , whose extended globally rigid graph is H_n . Without loss of generality, this move connects a new vertex v_{n+1} with the vertices v_1, v_2, v_3 . Let u be a neighbour of v_1 in G_{n+1} such that $v_2 \neq u \neq v_3$. The edge uv_1 exists also in G_n and H_n . If we set $H'_{n+1} = (H_n \cup \{v_1v_{n+1}, v_2v_{n+1}, v_3v_{n+1}, uv_{n+1}\}) -$

$\{v_1u\}$, then H'_{n+1} is globally rigid, because it is constructed from H_n by an H2 step. Hence, $H_{n+1} = H'_{n+1} \cup \{uv_{n+1}\}$ is also globally rigid, proving the statement in the case of H1 steps.

As for H3 steps, both H3x and H3v can be seen as an H2 step followed by an edge deletion. Extending the graph with the second deleted edge preserves global rigidity. \square

We can extend this result to minimally rigid graphs in arbitrary dimension constructed by appropriate generalizations of Henneberg steps H1, H2 or H3. As we mentioned, the lemma gives only an estimate for the smallest number of variables. It guarantees neither that such subsystem exists in every Cayley-Menger matrix of a minimally rigid graph (in fact we have found graphs with 8 or more vertices with no such a subsystem), nor that the solutions of the subsystem totally define the whole system. On the other hand, if such a subsystem exists, it can definitely give an upper bound.

An example is the 7-vertex graph G_{48} with the maximal number of embeddings ($r_3(G_{48}) = 48 = r_3(7)$, see Section 4). The labeling of the vertices is in Figure 2. There are 5 different square systems in 3 variables that completely define the mechanism. We can choose one of them involving only x_1, x_2, x_3 :

$$CM_{G_{48}} = \begin{pmatrix} 0 & 1 & 1 & 1 & 1 & 1 & 1 & 1 \\ 1 & 0 & d_{12}^2 & d_{13}^2 & d_{14}^2 & d_{15}^2 & d_{16}^2 & x_1 \\ 1 & d_{21}^2 & 0 & d_{23}^2 & x_2 & x_3 & d_{26}^2 & d_{27}^2 \\ 1 & d_{31}^2 & d_{32}^2 & 0 & d_{34}^2 & x_4 & x_5 & d_{37}^2 \\ 1 & d_{41}^2 & x_2 & d_{43}^2 & 0 & d_{45}^2 & x_6 & d_{47}^2 \\ 1 & d_{51}^2 & x_3 & x_4 & d_{54}^2 & 0 & d_{56}^2 & d_{57}^2 \\ 1 & d_{61}^2 & d_{62}^2 & x_5 & x_6 & d_{65}^2 & 0 & d_{67}^2 \\ 1 & x_1 & d_{72}^2 & d_{73}^2 & d_{74}^2 & d_{75}^2 & d_{76}^2 & 0 \end{pmatrix}.$$

One advantage of this approach is that we have much less equations compared with the sphere equations approach. In this example, we need a system of only 3 equations for the distance system, while 16 equations are required otherwise. Additionally, every solution of the distance system corresponds to two reflected embeddings. Hence, polynomial homotopy solvers are much faster in this case.

We can also apply algebraic elimination to reformulate this determinantal variety. We noticed that even the graph extended only with the edge v_1v_7 corresponding to the variables x_1 is globally rigid. This led us to compute the resultant of the square 3x3 system for x_1 , which can be obtained by repeated Sylvester resultants, Macaulay resultant and sparse resultant method with the same result. In order to specify the realizations, we also need the set of inequalities. There are 35 triangular inequalities and the same number of tetrahedral inequalities for the whole set of

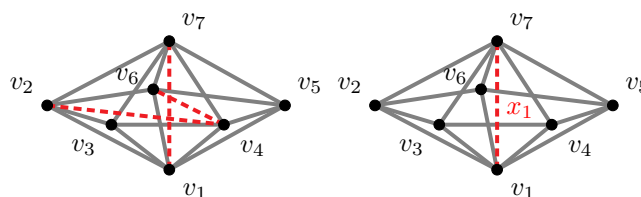


Figure 2: The graph G_{48} (grey edges). There are submatrices of $CM_{G_{48}}$ that involve only variables corresponding to the 3 red dashed edges of the left graph. The graph G_{48} extended by the edge v_1v_7 (that corresponds to the variable x_1) is globally rigid.

variables. Since we need to embed only one new edge, we are restricted to find the inequalities for x_1 . There are ten inequalities that include only x_1 (5 triangular and 5 tetragonal).

On the other hand, we detected graphs for which the subsystems do not fully describe the determinantal variety, since the number of solutions of the whole (overconstrained) system is smaller than this of the (square) subsystem for some generic choices of lengths. We conclude that the drawback of the method is that there is not a 1-1 correspondence between subsystems and global rigidity. Despite this fact, they seem better candidates for tight upper bound mixed volume computations.

3 Increasing the number of real embeddings

To improve $r_3(G)$ bounds, our first goal was to prove that $r_3(G_{48}) = c_3(G_{48})$. Initially we used methods already applied to increase the number of real solutions of a given polynomial system. We present a short overview of this approach.

Stochastic methods A first idea was to use stochastic sampling. Generic configurations of G_{48} embeddings in \mathbb{R}^3 were perturbed following the sampling methods presented in [9]. Applying this approach, it was straightforward to find configurations with $r_3(G_{48}, \mathbf{d})$ being equal to 16, 20 or 24. Our best result was $r_3(G_{48}, \mathbf{d}) = 32$.

Parametric searching with CAD method Maple's subpackage `RootFinding [Parametric]` implements Cylindrical Algebraic Decomposition principles for semi-algebraic sets [20]. This implementation could not work for the system of sphere equations, but was efficient using the semi-algebraic distance system. The algorithm can separate variables and parameters for every equation and give as output a decomposition of the space of parameters up to the number of solutions. In our case, it was possible to use only one parameter due to computational constraints, so all the other distances were fixed (our Maple worksheet is available at [19]).

It was again straightforward to find 24 embeddings even from totally random conformations. To get more we needed to exploit the symmetry of G_{48} , constructing non-generic flexible frameworks. Perturbing the lengths by a small quantity, $r_3(G_{48}, \mathbf{d})$ was again finite. Afterwards, we considered multiple edge lengths as linear combinations of the same parameter. Eventually, applying parameter searching, we were able to find lengths $\bar{\mathbf{d}}$ such that $r_3(G_{48}, \bar{\mathbf{d}}) = 28$:

$$\begin{aligned}
 \bar{d}_{12} &= 1.99993774567597, & \bar{d}_{27} &= 10.5360917228793, \\
 \bar{d}_{13} &= 1.99476987780024, & \bar{d}_{37} &= 10.5363171636461, \\
 \bar{d}_{14} &= 2.00343646098439, & \bar{d}_{47} &= 10.5357233031495, \\
 \bar{d}_{15} &= 2.00289249524296, & \bar{d}_{57} &= 10.5362736599978, \\
 \bar{d}_{16} &= 2.00013424746814, & \bar{d}_{67} &= 10.5364788463527, \\
 \bar{d}_{23} &= 0.99961432208948, & \bar{d}_{34} &= 1.00368644488060, \\
 \bar{d}_{45} &= 1.00153014850485, & \bar{d}_{56} &= 0.99572361653574, \\
 \bar{d}_{26} &= 1.00198771097407
 \end{aligned} \tag{1}$$

While this result was lower than the one achieved by stochastic searching, it had some promising properties (variables are taken from the determinantal variety of $CM_{G_{48}}$). Namely, all the solutions for x_1, x_2, x_3 are real, for x_1 even positive, and the x_1 solutions which are not embeddable are very close to the intervals imposed by the triangular and tetragonal inequalities.

Gradient Descent An algorithm that increases step by step the number of real embeddings is proposed in [8]. This method is based on gradient descent optimization, minimizing the

imaginary part of solutions, while forcing existing real roots to remain real via a semidefinite relation.

We applied it to the G_{48} sphere equations and a variant of it for distance equations starting from the optimal configurations found with the two previous approaches. In the first iterations the results were encouraging, but finally we could not generate more real embeddings.

The previous results motivated us to search other ways to achieve our first goal. Inspired by coupler curve visualization, we introduce an iterative procedure that modifies edge lengths so that the number of real embeddings might increase. In particular, it allows to find edge lengths to prove that $r_3(G) = c_3(G)$ for G_{48} and also other 7-vertex graphs G . At each iteration, only lengths of 4 edges in a specific subgraph are changed. One can be changed freely, whereas the other 3 are related. For this two-parametric family, we search values with the maximal number of embeddings globally.

3.1 Coupler curve

For a minimally rigid graph G , removing an edge uc yields a framework $H = (V_G, E_G \setminus uc)$ with one degree of freedom. If we fix a triangle containing u in order to avoid rotations and translations of H , then the vertex c draws the so called *coupler curve* under all possible motions of H . This idea was already used in [5] for obtaining 24 real embeddings of Desargues (3-prism) graph in \mathbb{R}^2 . A modification into \mathbb{R}^3 is straightforward – the number of embeddings of G corresponds to the number of intersection of the coupler curve of c of the graph H with a sphere centered at u with radius d_{uc} . The following definition recalls the concept of coupler curve more precisely.

Definition 2. *Let H be a graph with edge lengths $\mathbf{d} = (d_e)_{e \in E_H}$ and $v_1, v_2, v_3 \in V_H$ be such that $v_1v_2, v_2v_3, v_1v_3 \in E_H$. If the set $S_{\mathbb{R}}(H, \mathbf{d}, v_1v_2v_3)$ is one dimensional and $c \in V_H$, then the set*

$$\mathcal{C}_{c, \mathbf{d}} = \{(x_c, y_c, z_c) : ((x_v, y_v, z_v))_{v \in V_H} \in S_{\mathbb{R}}(H, \mathbf{d}, v_1v_2v_3)\}$$

is called a coupler curve of c w.r.t. the fixed triangle $v_1v_2v_3$.

Obviously, for given lengths \mathbf{d} of the graph H , we may vary the length d_{uc} of the removed edge uc so that the number of intersections of the coupler curve $\mathcal{C}_{c, \mathbf{d}}$ with the sphere centered at u with radius d_{uc} , i.e., the number of embeddings of G , is maximal. The following lemma enables us to move also the center of the sphere within a certain one-parameter family without changing the coupler curve.

Lemma 2. *Let G be a minimally rigid graph and let u, v, w, p, c be vertices of G such that $pv, vw \in E$ and the neighbours of u in G are v, w, p and c . Let $\mathcal{C}_{c, \mathbf{d}}$ be the coupler curve of c of the graph $H = (V_G, E_G \setminus \{uc\})$ with edge lengths $\mathbf{d} = (d_e)_{e \in E_H}$ w.r.t. the fixed triangle vuw . Let z_p be the altitude of p in the triangle uwp with lengths given by \mathbf{d} . The set $\{y_p : ((x_{v'}, y_{v'}, z_{v'}))_{v' \in V_H} \in S_{\mathbb{R}}(H, \mathbf{d}, vuw)\}$ has only one element y'_p . If the parametric edge lengths $\mathbf{d}'(t)$ are given by*

$$\begin{aligned} d'_{uw}(t) &= \|(x_w, y_w - t, 0)\|, & d'_{up}(t) &= \|(0, y'_p - t, z_p)\|, \\ d'_{uv}(t) &= t, & \text{and } d'_e(t) &= d_e \text{ for all } e \in E_H \setminus \{uv, uw, up\}, \end{aligned}$$

then the coupler curve $\mathcal{C}_{c, \mathbf{d}'(t)}$ of c w.r.t. the fixed triangle vuw is the same for all $t \in \mathbb{R}_+$, namely, it is $\mathcal{C}_{c, \mathbf{d}}$. Moreover, if $cw \in E_G$, then $\mathcal{C}_{c, \mathbf{d}'(t)}$ is a spherical curve.

Proof. Within this proof, all coupler curves are w.r.t. the triangle vuw . The situation is illustrated by Figure 3. Since G is minimally rigid, removing the edge uc yields a graph H such that $S_{\mathbb{R}}(H, \mathbf{d}, vuw)$ is one dimensional for a generic choice of \mathbf{d} . The set $\{y_p : ((x_{v'}, y_{v'}, z_{v'}))_{v' \in V_H} \in$

$S_{\mathbb{R}}(H, \mathbf{d}, vuw)$ has indeed only one element, since the coupler curve $\mathcal{C}_{p,\mathbf{d}}$ of p is a circle whose axis of symmetry is the y -axis. The parametric edge lengths $\mathbf{d}'(t)$ are such that the position of v and w is the same for all t . Moreover, the coupler curve $\mathcal{C}_{p,\mathbf{d}'(t)}$ of p is independent on t . Hence, the coupler curve $\mathcal{C}_{c,\mathbf{d}'(t)}$ is independent on t , because the only vertices adjacent to u in H are p, v and w , i.e., the position of u does not influence positions of the other vertices. \square

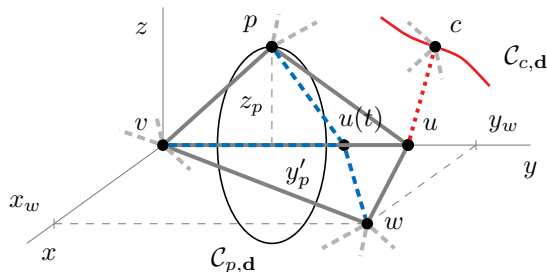


Figure 3: Since the lengths of up and uw are changed accordingly to the length of uv (blue dashed edges), the coupler curves $\mathcal{C}_{p,\mathbf{d}'(t)}$ and $\mathcal{C}_{c,\mathbf{d}'(t)}$ are independent on t . The red dashed edge uc is removed from G .

Thus, for every subgraph of G given by vertices u, v, w, p, c such that $pv, vw \in E$ and the neighbours of u in G are v, w, p and c , we have a two-parametric family of lengths $\mathbf{d}(t, r)$ such that the coupler curve $\mathcal{C}_{c,\mathbf{d}(t,r)}$ w.r.t. the fixed triangle vuw is the same for all t and r , where the parameter t determines lengths of uv, uw and up , and the parameter r represents the length of uc . Within this family, we look for values of t and r that maximize the number of embeddings.

We illustrate the method on the example of G_{48} . Let $\bar{\mathbf{d}}$ be edge lengths given by (1). We developed a program [19] that plots (using `Matplotlib` [16]) the coupler curve of the vertex v_6 of G with the edge v_2v_6 removed w.r.t. the fixed triangle $v_1v_2v_3$. Figure 4 is created by this program. There are 28 embeddings for $\bar{\mathbf{d}}$, but we can find position and radius of the sphere corresponding to the removed edge v_2v_6 such that there are 32 embeddings by using Lemma 2 for the subgraph $(u, v, w, p, c) = (v_2, v_3, v_1, v_7, v_6)$. This is obtained by setting

$$d_{12} = 4.0534, \quad d_{27} = 11.1069, \quad d_{26} = 3.8545, \quad d_{23} = 4.0519. \quad (2)$$

3.2 Sampling

Although edge lengths of G_{48} with 48 real embeddings can be obtained by manual application of Lemma 2 based on plots of coupler curves, we also implemented a program [19] that searches for a good position and radius of the sphere by sampling the parameters. The method and its implementation work also for minimally rigid graphs other than G_{48} .

We assume that the edge cw is present for a suitable subgraph (actually, this is the case for all suitable subgraphs of G_{48}). Thus, the coupler curve is spherical and the intersections of the coupler curve with the sphere representing the removed edge uc lies on the intersection of these two spheres, which is a circle. Hence, instead of sampling t and r , we sample circles on the sphere containing the coupler curve.

Since the sphere of the coupler curve is centered at w and the intersecting sphere has center at u , the center of the intersection circle is on the line uw and the plane of the circle is perpendicular to this line. Hence, the circle is determined by the angle $\varphi \in (-\pi/2, \pi/2)$ between the

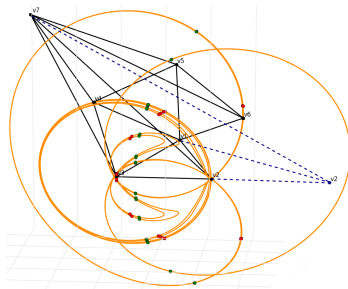


Figure 4: Coupler curve $\mathcal{C}_{v_6, \bar{d}}$ of G_{48} with the edge $v_2 v_6$ removed. The 28 red points are intersections of $\mathcal{C}_{v_6, \bar{d}}$ with the sphere centered at v_2 with edge lengths \bar{d} , whereas the 32 green ones are for edge lengths given by equation (2) (illustrated by blue dashed lines).

altitude of w in the triangle uvw and the line uw , and by the angle $\theta \in (0, \pi)$ between uw and cw , see Figure 5. Thus, we sample φ and θ in their intervals, compute t and r from their values and select edge lengths with the highest number of real embeddings. The algebraic systems are solved by polynomial homotopy continuation using the Python package `phcpy` [30]. In `phcpy`, one can specify a starting system with the set of its solutions instead of letting the program to construct it. Since the parameters change only slightly during the sampling, tracking the solutions of a new system from the solutions of the previous one is significantly faster than solving from scratch.

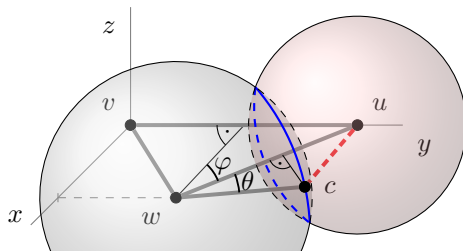


Figure 5: For fixed position of v and w , the angle φ determines the position of u , since u lies on the y -axis. If also the length of cw is given, then θ determines the length of uc . The intersection circle is blue.

3.3 More subgraphs suitable for sampling

Usually, one iteration of the sampling produces many edge lengths with the same number of real embeddings. If this number is not the desired one, then we need to pick starting edge lengths for the next iteration with a different subgraph suitable for sampling. Our heuristic choice is based on clustering of pairs (φ, θ) using the function `DBSCAN` from the `sklearn` Python package [23]. From each cluster, we pick the center of gravity as (φ, θ) for the output lengths, or the pair (φ, θ) closest to this center if the edge lengths corresponding to the center have less real embeddings.

We tested two approaches in sampling for subgraphs:

1. *Tree search* – we apply the procedure using all suitable subgraphs for given starting lengths

and then we do the same recursively for all outputs whose number of embeddings increased until the required number is reached (or there are no increments). We trace the state tree depth-first.

2. *Linear search* – we order all suitable subgraphs and an output from the procedure applied to starting lengths with the first subgraph is used as input for the procedure with the second subgraph, etc. There is also branching because of multiple clusters – we test all of them in depth-first way.

4 Classification and Lower Bounds

Henneberg steps may result in isomorphic graphs either constructed by the same H-step or by another one. We recall that no H3x or H3v step is needed for 7 and 8-vertex graphs. We classify each graph up to isomorphism by the sequence of Henneberg steps needed for its construction. We use a certain hierarchy for this classification: on the one hand there are graphs that can be constructed by an H1 move in the last step, while for the others H2 is needed. This process is important, since H1 steps trivially double the number of real embeddings as the new vertex lies in the intersection of 3 spheres. This means that the number of embeddings for H1 graphs is already known, assuming that we know the number for the parent graph. Our `MATLAB` and `SageMath` implementations, which verify each other, were used to apply Henneberg steps and remove isomorphisms (see [19]). This is not a computationally difficult task for $n = 7$ or 8. We remark that this is also done in [15] up to 10 vertices.

The first estimate of $c_3(G)$ is the mixed volume of the algebraic systems. Let f be a square polynomial system in m variables. The convex hull of the exponents vector of each polynomial is its Newton polytope. The mixed volume of the polytope bounds the number of solutions and is tight generically in $(\mathbb{C}^*)^m$. We computed the mixed volume for both sphere and distance equations. We solved the systems for random edge lengths and checked whether the mixed volume bound was tight in all cases. Finally, we used the method in Section 3 to find parameters maximizing the number of real embeddings.

4.1 7-vertex graphs

For $n = 6$, there are three H1 graphs and one obtained with an H2 step – the cyclohexane G_{16} . The number of real embeddings of the H1 graphs is 8, while it is known that $r_3(G_{16}) = 16$ [10]. One can also obtain lengths \mathbf{d} such that $r_3(G_{16}, \mathbf{d}) = 16$ by our method within a few tries with random starting lengths.

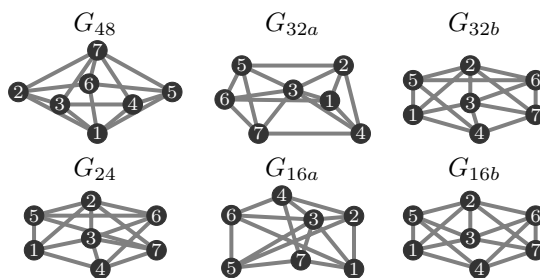


Figure 6: All 7-vertex graphs constructed only by an H2 move in the last step.

Using Henneberg steps, we tackle the case $n = 7$. There are 18 graphs constructed using a sequence of only H1 steps, while two are obtained if we apply H1 to G_{16} . Hence, the number of real embeddings is 16, resp. 32, by the doubling argument. Moreover, there are 6 graphs obtained by H2 on a 6-vertex graph, see Figure 6. See [19] for the full list.

The results (mixed volume for both systems, numbers of complex and real embeddings) for these 6 graphs are in Table 1. These results give a full classification of the embeddings of all 7-vertex minimally rigid graphs in \mathbb{R}^3 . We present edge lengths for all these graphs proving that all embeddings can be real, i.e., $r_3(G) = c_3(G)$.

Graph	G_{48}	G_{32a}	G_{32b}	G_{24}	G_{16a}	G_{16b}
MV sphere eq.	48	32	32	32	32	32
MV dist. subsyst.	48	32	32	24	24	16
$c_3(G)$	48	32	32	24	16	16
$r_3(G)$	48	32	32	24	16	16

Table 1: Mixed volume (MV) and number of solutions for 7-vertex graphs constructed only by H2 in the last step.

There are 20 subgraphs of G_{48} given by vertices (u, v, w, p, c) satisfying the assumption in Lemma 2, that is, they are suitable for the sampling procedure. Using tree search approach, we obtained \mathbf{d} such that $r_3(G_{48}, \mathbf{d}) = 48$ in only 3 steps (starting from $\bar{\mathbf{d}}$ and using subgraphs $(v_5, v_6, v_1, v_7, v_4)$, $(v_4, v_3, v_1, v_7, v_5)$ and $(v_3, v_2, v_1, v_7, v_4)$):

$$\begin{array}{llll}
d_{12} = 1.9999, & d_{16} = 2.0001, & d_{45} = 7.0744, & d_{47} = 11.8471, \\
d_{13} = 1.9342, & d_{26} = 1.0020, & d_{56} = 4.4449, & d_{57} = 11.2396, \\
d_{14} = 5.7963, & d_{23} = 0.5500, & d_{27} = 10.5361, & d_{67} = 10.5365. \\
d_{15} = 4.4024, & d_{34} = 5.4247, & d_{37} = 10.5245, &
\end{array}$$

For other graphs constructed only by an H2 move in the last step we used various starting lengths, we just list the edge lengths that give the appropriate maximal number of real embeddings:

$$\begin{array}{llll}
G_{16a} : & d_{13} = 5.75, & d_{56} = 7.90, & d_{16} = 8.48, \\
d_{37} = 5.91, & d_{25} = 7.15, & d_{35} = 5.09, & d_{12} = 4.36, \\
d_{46} = 8.78, & d_{57} = 10.22, & d_{36} = 7.06, & d_{17} = 3.77, \\
d_{47} = 7.19, & d_{23} = 3.81, & d_{34} = 3.23, & d_{24} = 6.05. \\
G_{16b} : & d_{47} = 4.46, & d_{26} = 7.47, & d_{45} = 7.72, \\
d_{14} = 6.51, & d_{13} = 3.53, & d_{23} = 7.69, & d_{37} = 5.76, \\
d_{25} = 9.48, & d_{35} = 6.10, & d_{12} = 4.62, & d_{67} = 3.09, \\
d_{27} = 5.90, & d_{46} = 7.07, & d_{15} = 5.69, & d_{36} = 6.43.
\end{array}$$

G_{24} :	$d_{47} = 5.65,$	$d_{26} = 5.70,$	$d_{56} = 4.70,$
$d_{14} = 8.33,$	$d_{13} = 4.77,$	$d_{23} = 10.31,$	$d_{37} = 7.10,$
$d_{25} = 9.32,$	$d_{12} = 11.05,$	$d_{46} = 6.49,$	$d_{57} = 5.77,$
$d_{27} = 6.00,$	$d_{15} = 9.40,$	$d_{36} = 8.57,$	$d_{34} = 7.64.$
G_{32a} :	$d_{13} = 6.27,$	$d_{56} = 9.23,$	$d_{14} = 8.06,$
$d_{23} = 8.83,$	$d_{37} = 5.62,$	$d_{25} = 9.74,$	$d_{35} = 5.60,$
$d_{12} = 10.95,$	$d_{67} = 9.28,$	$d_{57} = 7.88,$	$d_{36} = 8.26,$
$d_{47} = 8.74,$	$d_{16} = 11.56,$	$d_{34} = 6.11,$	$d_{24} = 8.95.$
G_{32b} :	$d_{47} = 85.49,$	$d_{26} = 7.11,$	$d_{56} = 22.08,$
$d_{14} = 87.33,$	$d_{13} = 10.81,$	$d_{23} = 4.47,$	$d_{37} = 7.10,$
$d_{25} = 20.70,$	$d_{12} = 11.06,$	$d_{67} = 9.29,$	$d_{15} = 21.49,$
$d_{27} = 7.68,$	$d_{45} = 78.53,$	$d_{36} = 7.53,$	$d_{34} = 84.17.$

4.2 8-vertex graphs

We repeated our methods for $n = 8$. There are 311 graphs that can be constructed by an H1 step (hence, $r_3(G)$ is known by H1 doubling argument), while 63 require an H2 step. So we computed only the complex bounds of the latter: 58 of them have 96 complex embeddings or less, one has 112 complex embeddings, 3 have 128 complex embeddings and there is a unique graph G_{160} with 160 complex embeddings.

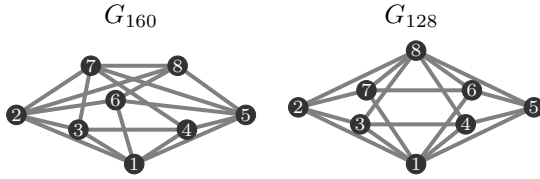


Figure 7: G_{160} has the maximal number of complex embeddings (160). We proved that $r_3(G_{128}) = 128$.

We were interested in improving the lower bound established previously. No graph with less than 128 embeddings could improve the bound obtained by G_{48} . Thus, we applied the technique to maximize real embeddings on two different 8-vertex graphs: G_{160} and G_{128} , see Figure 7. Both can be constructed by H2 step from G_{48} , and the structure of G_{128} is similar to G_{48} . Therefore, we use some lengths of G_{48} with many embeddings for the common edges for the starting lengths. The following edge lengths of G_{128} with 128 real embeddings were found by the algorithm:

$d_{12} = 8.7093,$	$d_{17} = 2.1185,$	$d_{68} = 10.5532,$	$d_{56} = 0.7536,$
$d_{13} = 10.3433,$	$d_{28} = 13.5773,$	$d_{78} = 10.5509,$	$d_{67} = 1.5449,$
$d_{14} = 1.9373,$	$d_{38} = 14.6173,$	$d_{23} = 13.5267,$	$d_{27} = 9.2728.$
$d_{15} = 1.9379,$	$d_{48} = 10.5237,$	$d_{34} = 10.1636,$	
$d_{16} = 2.0691,$	$d_{58} = 10.5237,$	$d_{45} = 0.0634,$	

For G_{160} we have obtained lengths for 132 real embeddings:

$$\begin{array}{llll}
d_{12} = 1.999, & d_{23} = 1.426, & d_{37} = 10.447, & d_{58} = 4.279, \\
d_{13} = 1.568, & d_{26} = 0.879, & d_{45} = 7.278, & d_{68} = 0.398, \\
d_{14} = 6.611, & d_{27} = 10.536, & d_{47} = 11.993, & d_{78} = 10.474. \\
d_{15} = 4.402, & d_{28} = 0.847, & d_{56} = 4.321, & \\
d_{16} = 1.994, & d_{34} = 6.494, & d_{57} = 11.239, &
\end{array}$$

More values for edge lengths of the presented graphs with various number of embeddings are available in [19]. We remark that it takes only few seconds to construct all Geiringer graphs up to 8 vertices and compute their mixed volumes. Complex embeddings computation takes approximately 1 second for one 7-vertex graph and 4 seconds for an 8-vertex graph. Although we take advantage of tracking solutions in our implementation of the sampling method (which speeds up the computation significantly), the time of sampling for G_{160} takes about 8 hours using 8 cores (this time strongly depends on the starting lengths). In order to get the lengths with 132 embeddings, we tested about 200 different starting conformations.

4.3 Lower bounds

To compute a lower bound on the maximum number of embeddings for rigid graphs in the space with n vertices, we use as a building block a rigid graph G with low $|V_G|$, but high $r_3(G)$. To do so, we need the following theorem from [15]:

Theorem 1. *Let G be a rigid graph, with a rigid subgraph H . We construct a rigid graph using k copies of G , where all the copies have the subgraph H in common. The new graph is rigid, has $n = |V_H| + k(|V_G| - |V_H|)$ vertices, and the number of its real embeddings is at least*

$$2^{(n-|V_H|) \bmod (|V_G|-|V_H|)} \cdot r_3(H) \cdot \left(\frac{r_3(G)}{r_3(H)} \right)^{\lfloor \frac{n-|V_H|}{|V_G|-|V_H|} \rfloor}.$$

If we use G_{160} as G and one of its triangle subgraphs as H , then we obtain the following lower bound.

Corollary 1. *The maximum number of real embeddings of rigid graphs in \mathbb{R}^3 with n vertices is bounded from below by*

$$2^{(n-3) \bmod 5} 132^{\lfloor (n-3)/5 \rfloor}.$$

The bound asymptotically behaves as 2.6553^n .

The previous lower bound was 2.51984^n [11], whereas using G_{48} as G gives 2.6321^n . It would be tempting to use as H a tetrahedron, say T , for which it holds $r_3(T) = 2$. Such a choice of a subgraph would have further improved the lower bound as the denominator of the exponent would have been smaller. Unfortunately, G_{48} , G_{128} , and G_{160} do not contain a tetrahedron as a subgraph.

5 Conclusion

By exploiting the (semi-)algebraic modeling of the embeddings of minimally rigid spatial graphs we present new classification results and a novel method to maximize $r_3(G)$. The latter led to improved lower bounds. Finding better asymptotic bounds is always an open question. A first step should be to find out the exact value of $r_3(G_{160})$. Furthermore, computations using our method for $n \geq 9$ may also give better results in this direction. Another direction is to find an efficient variant of our sampling method for other dimensions. Finally, subsystems of the determinantal varieties may improve the upper bounds for $c_3(G)$.

Acknowledgments This work is part of the project ARCADES that has received funding from the European Union’s Horizon 2020 research and innovation programme under the Marie Skłodowska-Curie grant agreement No 675789. ET is partially supported by ANR JCJC GALOP (ANR-17-CE40-0009) and the PGM0 grant GAMMA.

References

- [1] F. Bihan, J. M. Rojast, and F. Sottile. On the sharpness of fewnomial bounds and the number of components of fewnomial hypersurfaces. In *Algorithms in algebraic geometry*, pages 15–20. Springer, 2008.
- [2] F. Bihan and P.-J. Spaenlehauer. Sparse polynomial systems with many positive solutions from bipartite simplicial complexes. *arXiv:1510.05622*, 2016.
- [3] L. M. Blumenthal. *Theory and Applications of Distance Geometry*. Chelsea Publishing Company, New York, 1970.
- [4] C. S. Borcea. Point configurations and Cayley-Menger Varieties. *arXiv:math/0207110*, 2002.
- [5] C. S. Borcea and I. Streinu. The Number of Embeddings of Minimally Rigid Graphs. *Discrete & Computational Geometry 2*, page 287–303, 2004.
- [6] J. Capco, M. Gallet, G. Grasegger, C. Koutschan, N. Lubbes, and J. Schicho. The number of realizations of a laman graph. *SIAM Journal on Applied Algebra and Geometry*, 2(1):94–125, 2018.
- [7] R. Connelly. Generic global rigidity. *Discrete Comput. Geom.* 33, page 549–563, 2005.
- [8] P. Dietmaier. The stewart-gough platform of general geometry can have 40 real postures. *Advances in Robot Kinematics: Analysis and Control*, pages 1–10, 1998.
- [9] I. Z. Emiris and G. Moroz. The assembly modes of rigid 11-bar linkages. *IFTToMM 2011 World Congress, Jun 2011, Guanajuato, Mexico*, 2011.
- [10] I. Z. Emiris and B. Mourrain. Computer algebra methods for studying and computing molecular conformations. *Algorithmica* 25, pages 372–402, 1999.
- [11] I.Z. Emiris, E. Tsigaridas, and A. Varvitsiotis. Mixed volume and distance geometry techniques for counting euclidean embeddings of rigid graphs. *Distance Geometry: Theory, Methods and Applications*", edited by A. Mucherino, C. Lavor, L. Liberti and N. Maculan, pages 23–45, 2013.
- [12] D.G. Emmerich. *Structures Tendues et Autotendantes*. Ecole d’Architecture de Paris la Villette, 1988.
- [13] J.C. Faugere and D. Lazard. The combinatorial classes of parallel manipulators. *Mechanism & Machine Theory* 30(6), pages 765–776, 1995.
- [14] S. Gortler, A. Healy, and D. Thurston. Characterizing generic global rigidity. *Am. J. Math.* 132(4), pages 897–939, 2010.
- [15] G. Grasegger, C. Koutschan, and E. Tsigaridas. Lower bounds on the number of realizations of rigid graphs. *Experimental Mathematics*, pages 1–12, 2018.

- [16] J. D. Hunter. Matplotlib: A 2d graphics environment. *Computing In Science & Engineering*, 9(3):90–95, 2007.
- [17] B. Jackson and J.C. Owen. Equivalent realisations of rigid graphs. *10th Japanese-Hungarian Symposium on Discrete Mathematics and Its Applications*, pages 283–289, 2017.
- [18] B. Jackson and J.C. Owen. Equivalent realisations of a rigid graph. *Discrete Applied Mathematics*, 2018.
- [19] J. Legerský and E. Bartzos. Spatial graph embeddings and coupler curves – source code and results, 2018.
- [20] S. Liang, J. Gerhard, D. J. Jeffrey, and G. Moroz. A Package for Solving Parametric Polynomial Systems. *ACM Communications in Computer Algebra*, 43(3):61 – 72, 2009.
- [21] L. Liberti, B. Masson, J. Lee, C. Lavor, and A. Mucherino. On the number of realizations of certain henneberg graphs arising in protein conformation. *Discrete Applied Mathematics*, 165, page 213–232, 2014.
- [22] H. Maehara. On Graver’s Conjecture Concerning the Rigidity Problem of Graphs. *Discrete Comput Geom* 6, pages 339–342, 1991.
- [23] F. Pedregosa, G. Varoquaux, A. Gramfort, V. Michel, B. Thirion, O. Grisel, M. Blondel, P. Prettenhofer, R. Weiss, V. Dubourg, J. Vanderplas, A. Passos, D. Cournapeau, M. Brucher, M. Perrot, and E. Duchesnay. Scikit-learn: Machine learning in Python. *Journal of Machine Learning Research*, 12:2825–2830, 2011.
- [24] H. Pollaczek-Geiringer. Über die Gliederung ebener Fachwerke. *Zeitschrift für Angewandte Mathematik und Mechanik (ZAMM)*, 7(1):58–72, 1927.
- [25] H. Pollaczek-Geiringer. Zur Gliederungstheorie räumlicher Fachwerke. *Zeitschrift für Angewandte Mathematik und Mechanik (ZAMM)*, 12(6):369–376, 1932.
- [26] B. Schulze and W. Whiteley. *Rigidity and scene analysis*, chapter 61, pages 1593–1632. CRC Press LLC, 2017.
- [27] F. Sottile. Enumerative real algebraic geometry. In *Algorithmic and Quantitative Real Algebraic Geometry, DIMACS Series in Discrete Mathematics and Theoretical Computer Science, Volume 60*, AMS, pages 139–180, 2003.
- [28] R. Steffens and T. Theobald. Mixed volume techniques for embeddings of laman graphs. *Computational Geometry* 43, pages 84–93, 2010.
- [29] T.-S. Tay and W. Whiteley. Generating isostatic frameworks. *Topologie Structurale*, pages 21–69, 1985.
- [30] J. Verschelde. Modernizing phcpack through phcpy. In *Proceedings of the 6th European Conference on Python in Science (EuroSciPy 2013)*, pages 71–76, 2014.
- [31] D. Walter and M. L. Husty. On a 9-bar linkage, its possible configurations and conditions for paradoxical mobility. *IFTToMM World Congress, Besançon, France*, 2007.
- [32] D. Zelazo, A. Franchi, F. Allgöwer, H. H. Bühlhoff, and P.R. Giordano. Rigidity maintenance control for multi-robot systems. *Robotics: Science and Systems, Sydney, Australia*, 2012.
- [33] Z. Zhu, A.M.-C. So, and Y. Ye. Universal rigidity and edge sparsification for sensor network localization. *SIAM Journal on Optimization*, 20(6), page 3059–3081, 2010.